This journal is © The Royal Society of Chemistry 2012

Electronic Supplemental Information

Isabel Correia, Tamás Jakusch, Enoch Cobbinna, Sameena Mehtab, Isabel Tomaz, Nóra Nagy, Antal Rockenbauer, João Costa Pessoa and Tamás Kiss

Evaluation of the binding of oxovanadium(IV) to Human Serum Albumin

ESI 1 – Spectroscopic studies with fatted HSA and $V^{IV}O$

Figure ESI1-1 shows the CD spectra obtained in experiments containing fatted and defatted HSA (630□M) and $V^{IV}O$. These illustrate that the presence of fatty acids decrease the intensity of the CD spectra, probably due to disruption of the MBS site, where $V^{IV}O$ binds.

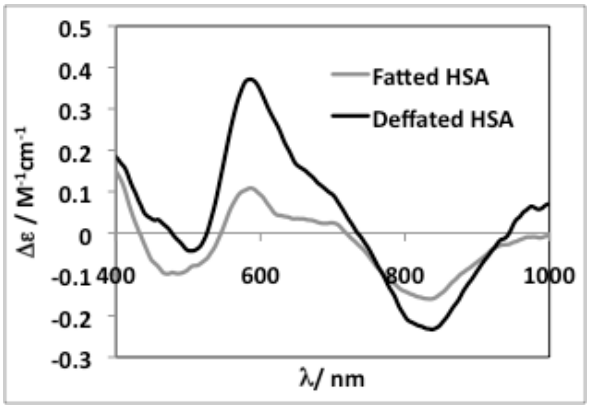

Figure ESI1-1 – CD spectra in the visible range of solutions containing 0.630□M of HSA and $V^{IV}O(ClO_4)_2$ with a ratio of HSA : $V^{IV}O$ = 1 : 5.

ESI 2 – Zn^{II} – $V^{IV}O$ competion studies for HSA binding

Figures ESI2-1 and ESI2-1 show the EPR spectra measured in the competition studies with Zn^{II}, with both fatted and defatted HSA, a HSA : $V^{IV}O$ ratio of 1 : 5 and different amounts of Zn^{II}.

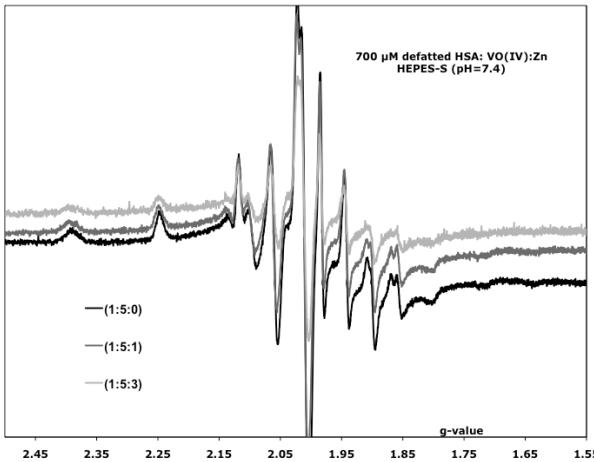

Figure ESI2-1 – First derivative X-band EPR spectra of solutions containing 0.700 µM of defatted HSA; a HSA:$V^{IV}O$ ratio = 1:5 and increasing amounts of Zn^{II} indicated in the figure.

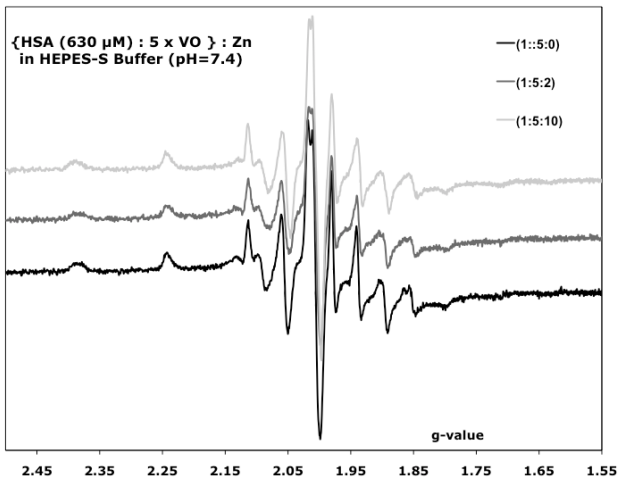

Figure ESI2-2 – First derivative X-band EPR spectra of solutions containing 0.650 μM of fatted HSA; a HSA:$V^{IV}O$ ratio = 1:5 and increasing amounts of Zn^{II} indicated in the figure.

The figures show that in both cases there is a small decrease in the EPR signal intensity after addition of Zn^{II}, but a significant amount of $V^{IV}O$ remains bound to the protein.

ESI 3 – The interaction of HSA with Cu^{II}

Although several authors have studied the HSA-Cu^{II} system we decided to reevaluate it by CD and EPR. Figure ESI3-1 shows the CD spectra measured for solutions containing 0.500 □M of HSA and different amounts of Cu^{II} at pH = 7.4 and the variation of the CD signal at several wavelengths.

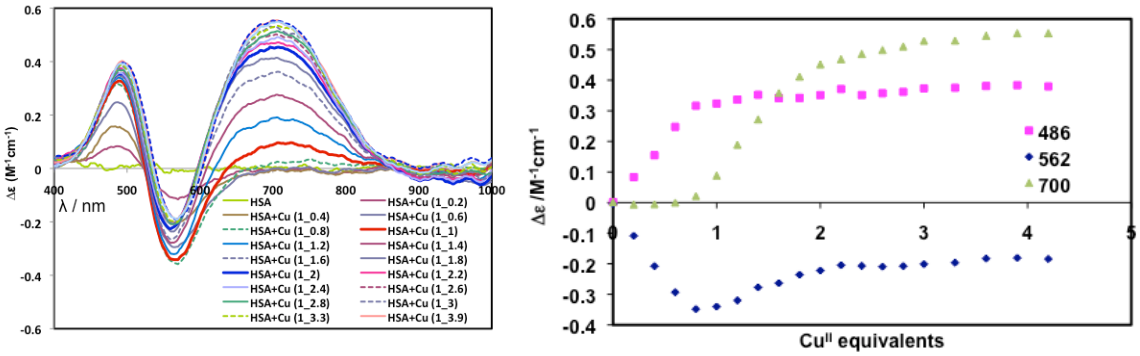

A **B**

Figure ESI3-1 – A) CD spectra in the visible range of solutions containing 0.500 μM of HSA titrated with Cu^{II}. The molar ratios are indicated in the figure. B) Variation of the Δε at different λ indicated in the figure.

These spectra were used to calculate the individual spectra of the two species formed in the system: Cu^{II} bound to the ATCUN site and Cu^{II} bound to the MBS site, which are shown in Figure ESI3-2. These confirm the assumptions made by other authors concerning the binding of Cu^{II} to HSA and the assignment of the CD bands.

This journal is © The Royal Society of Chemistry 2012

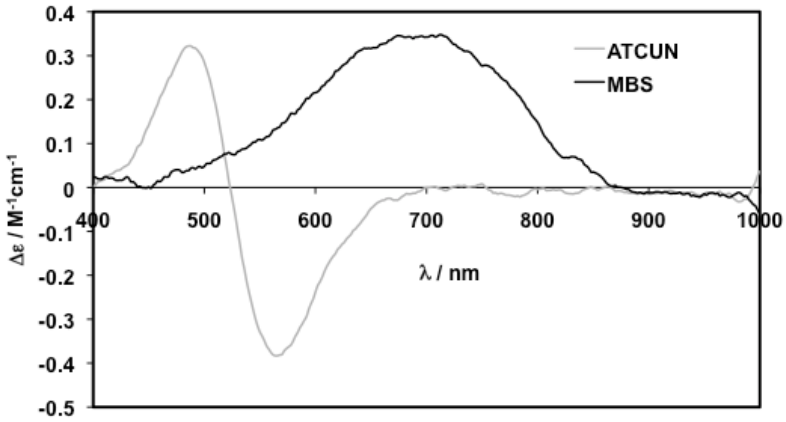

Figure ESI3-2 – Calculated CD spectra in the visible range for Cu^{II} coordinated at the ATCUN and MBS sites of HSA.

The X-band EPR spectra are depicted in figure ESI3-3 and show the presence of one species at HSA:Cu^{II} ratio of 1, and two species for Cu^{II}:HSA > 1. Super-hyperfine structure is detected in all spectra, due to the binding of HSA to the amide nitrogens of the ATCUN site.

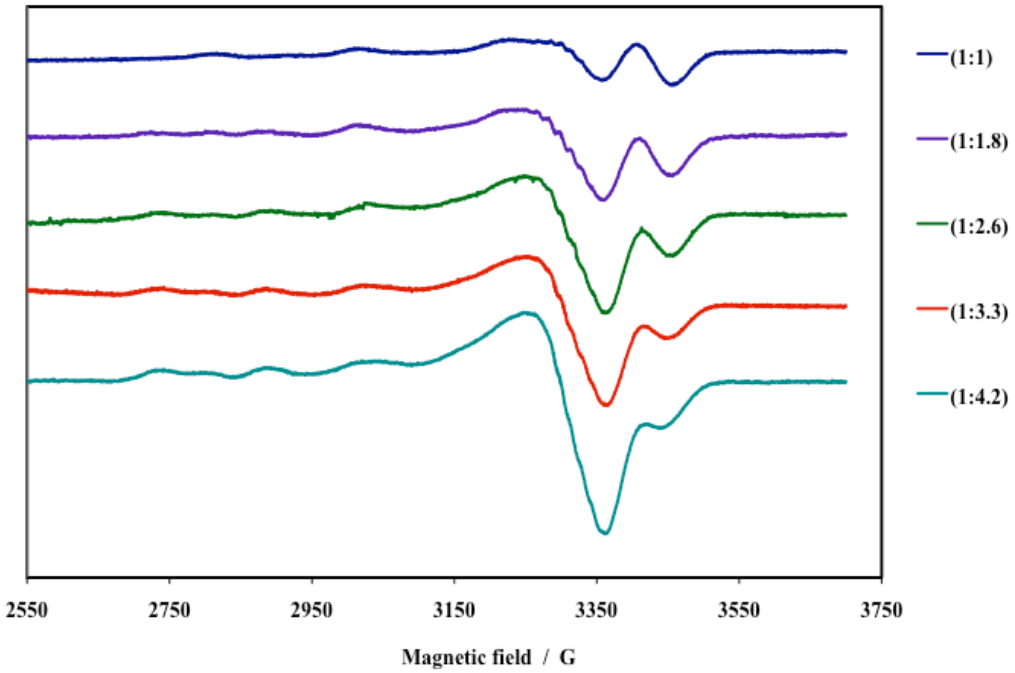

Figure ESI3-3 First derivative X-band EPR spectra of solutions containing 0.500 µM of HSA and increasing amounts of Cu^{II} indicated in the figure.

The changes observed in the X-band EPR spectra upon addition of $V^{IV}O$ to a solution containing HSA and Cu^{2+} with a molar ratio of 1:2 are shown in figure ESI3-4. The individual calculated EPR spectra for Cu^{II} coordinated at the ATCUN and MBS sites of HSA are depicted in Fig. ESI3-5.

This journal is © The Royal Society of Chemistry 2012

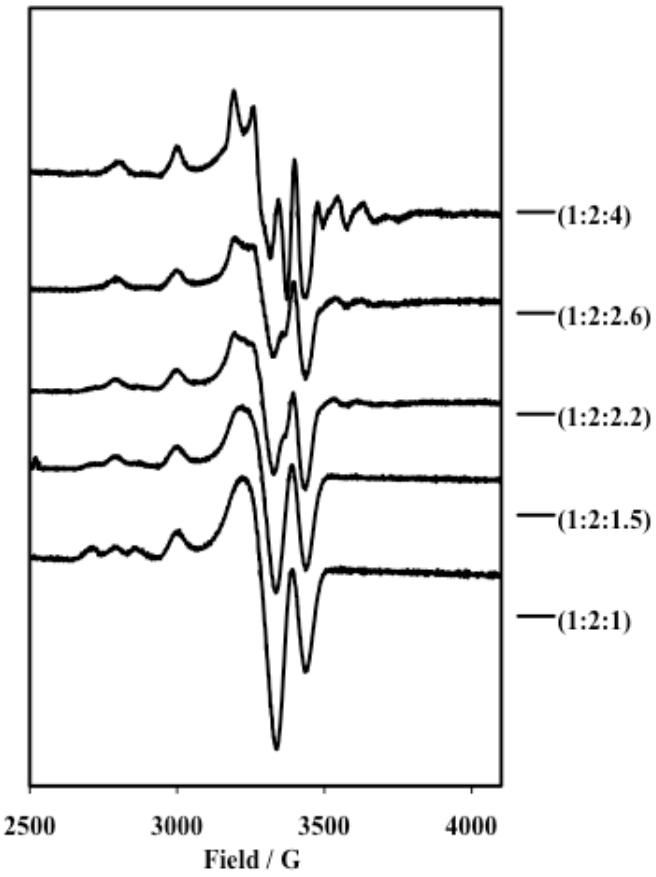

Figure ESI3-4 – First derivative X-band EPR spectra of solutions containing 0.600 µM of HSA and Cu^{2+}, with a HSA:Cu^{II} ratio = 1:2, and upon adding increasing amounts of $V^{IV}O$, which are indicated in the figure.

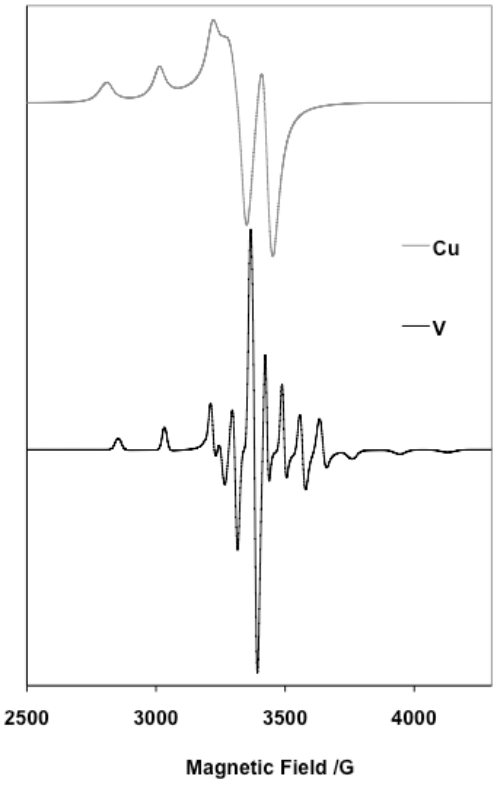

Figure ESI3-5 – Individual calculated Cu^{II} and $V^{IV}O$ EPR spectra for Cu^{II} and $V^{IV}O$ bound to HSA.

This journal is © The Royal Society of Chemistry 2012

ESI3-6 – Fitting of the X-band EPR spectra of solutions containing defatted HSA (0.50mM), $V^{IV}O$: HSA = 5 : 1 and increasing amounts of Cu^{II}

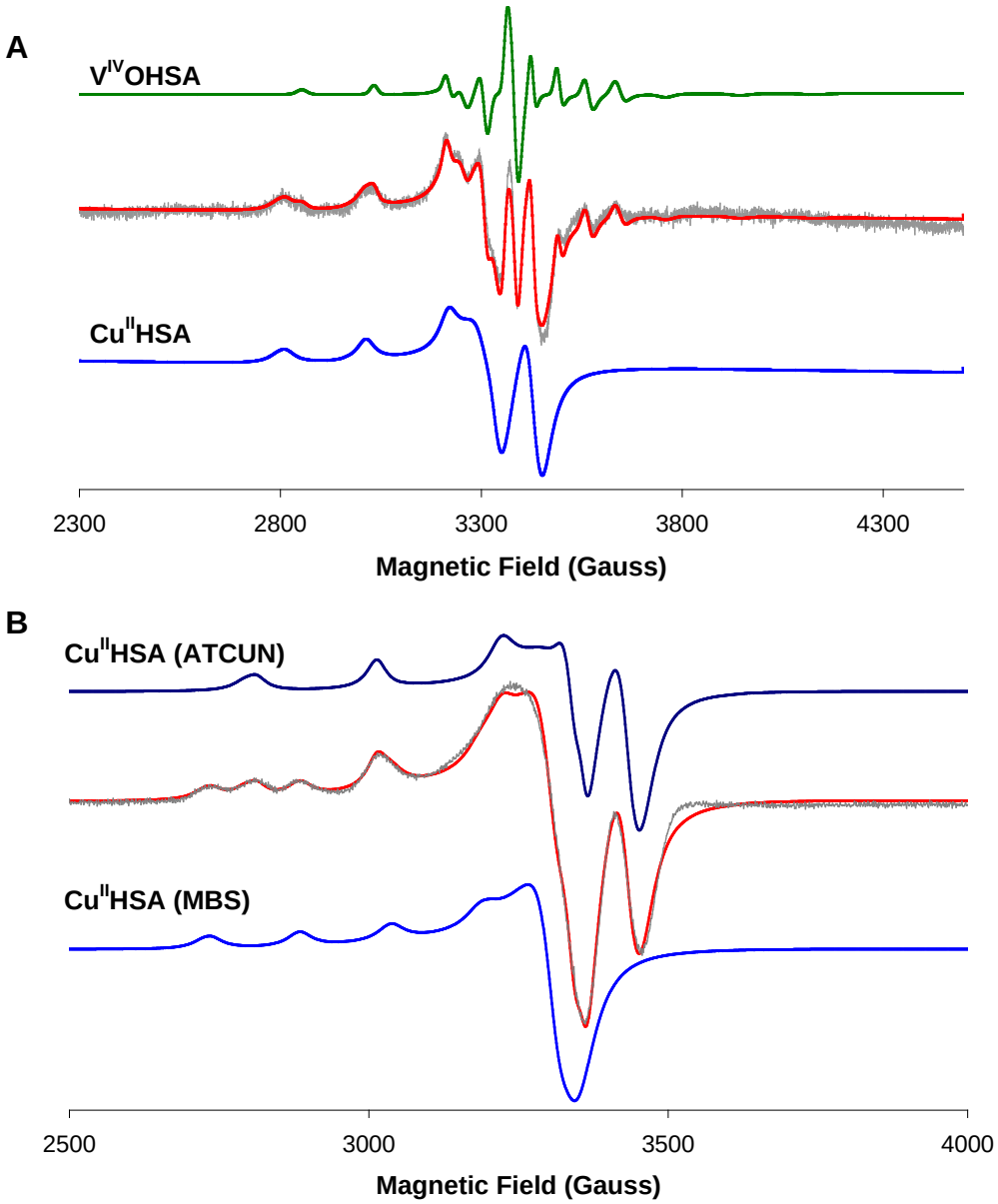

Figure ESI3-6 shows two example of the fitting of the EPR spectra obtained in experiments containing defatted HSA (630µM) and $V^{IV}O$ = 1 : 5 and increasing amounts of Cu^{II}. The exact ratios (HSA : $V^{IV}O$: Cu^{II}) **A** 1 : 5 : 1 **B** : 1 : 5 : 2 At the ratio 1 : 5 : 1 (HSA : $V^{IV}O$: Cu^{II}) only the $V^{IV}O$HSA and the Cu^{II}HSA (ATCUN) type spectra are observable.

At the ratio 1 : 5 : 2 (HSA : $V^{IV}O$: Cu^{II}) no $V^{IV}O$HSA type spectrum is observable. The ratio of the double integrated spectra of Cu^{II}HSA (ATCUN) and Cu^{II}HSA (MBS) is ~ 1 : 1.

Figure ESI3-7 depicts the CD spectrum in the visible range of a solution containing HSA, with HSA:$V^{IV}O$ = 1:5 at pH = 7.4, and the changes observed when Cu^{II} is added to this solution. The figure shows the CD spectra upon additions up to 1 mol equivalent of Cu^{II}.

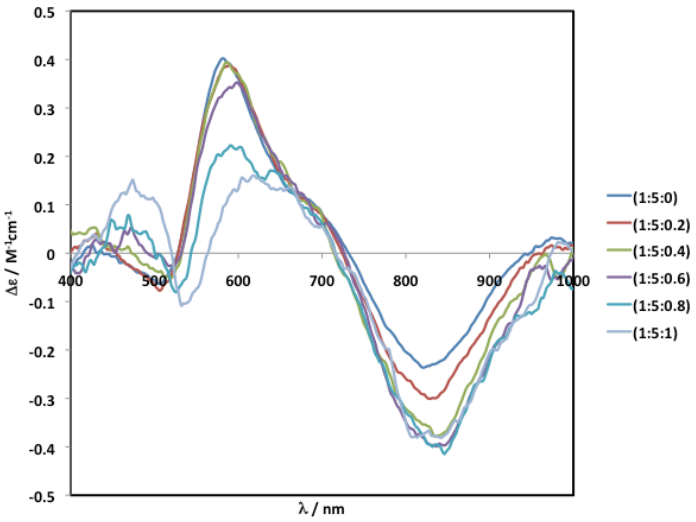

Figure ESI3-7 –CD spectra in the visible range of solutions containing 0.500 μM of HSA, HSA:$V^{IV}O$ = 1:5 and upon adding Cu^{2+} (Cu^{II} from 0 to 1 mol equivalents vs. HSA).

This journal is © The Royal Society of Chemistry 2012

ESI4 – Ternary systems

The X-band EPR spectra of solutions containing HSA, $V^{IV}O$ and maltol are depicted in figure ESI4-1. It is shown that upon adding maltol there is a strong increase in the EPR signal, corroborating our assumption that a significant part of the $V^{IV}O$ bound to HSA is present as EPR silent species. Upon addition of maltol, and its coordination to $V^{IV}O$ bound to HSA, a monomeric species is produced, with a much stronger EPR signal.

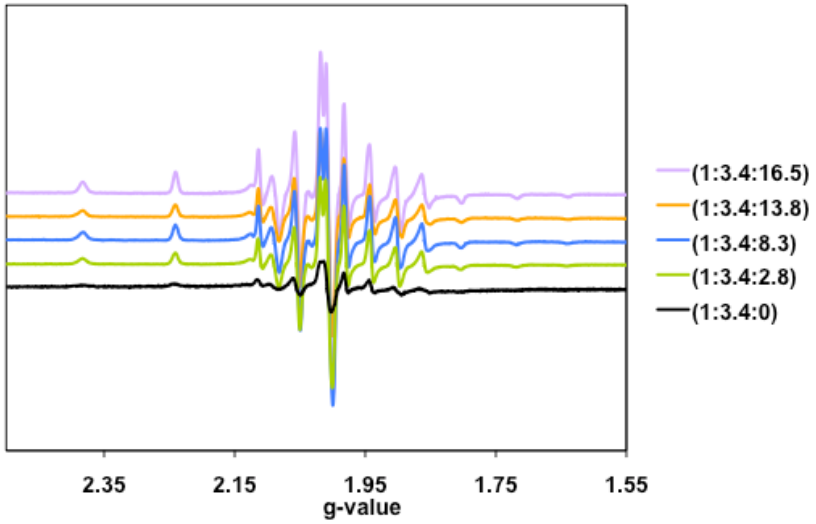

Figure ESI4-1 – First derivative X-band EPR spectra of solutions containing 0.630 µM of HSA, HSA:$V^{IV}O$ = 1:3.4 and upon progressively adding maltol (0 to 16.5 mol equivalents). The spectrum with (1:3.4:0) molar ratio was measured with a gain of $6.3x10^4$ and all other spectra with a slightly lower gain: $2.5x10^4$.

Figure ESI4-2 shows the CD spectra obtained after stepwise additions of Gly-L-His to a solution containing $V^{IV}O$ and maltol in a 1:2 molar ratio at pH=7.4. The resulting spectra are very similar to those obtained for solutions containing HSA instead of Gly-L-His (see e.g. Fig. ESI4-4), suggesting coordination of the metal complex to HSA by an imidazole N donor of a His residue. It is possible that the O_{amide} from the neighboring Gly residue also binds to V^{IV}. The EPR spectra shown in Fig ESI5-3 also corroborate this assumption since the main EPR-active species in the Gly-L-His system presents hyperfine parameters similar to those obtained in the HSA-$V^{IV}O$ system.

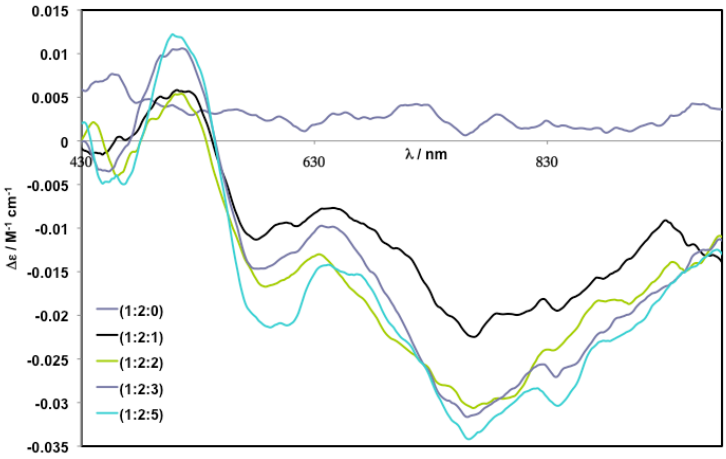

Figure ESI4-2 - CD spectra in the visible range of solutions containing $V^{IV}O$: maltol (1:2) and upon stepwise additions of Gly-L-His in HEPES-S buffer pH of 7.4. C_{VO} = 3 mM and the molar ratios are indicated in the figure.

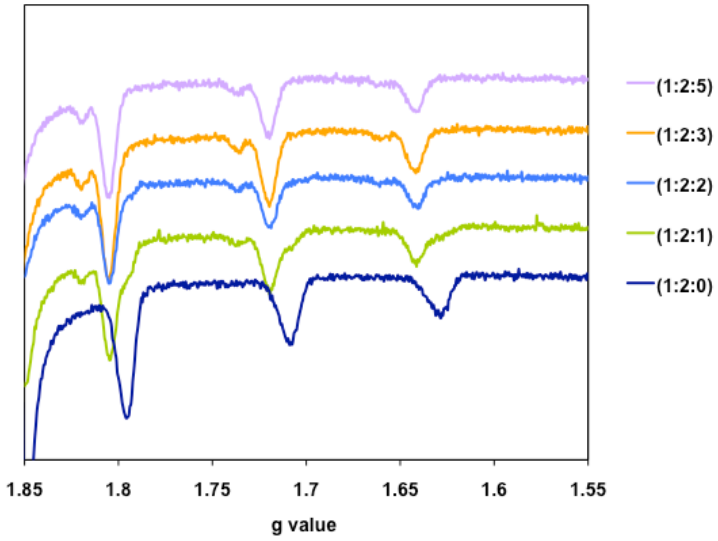

Figure ESI4-3 – High region of the X-band EPR spectra of the system $V^{IV}O$: maltol : Gly-His in HEPES-S buffer pH of 7.4. C_{VO} = 3 mM and the molar ratios are indicated in the figure.

If to solutions containing HSA at pH 7.4 maltol is added, no CD spectra is recorded for λ > 370 nm. Stepwise additions of:

- maltol to solutions containing HSA and $V^{IV}OSO_4$ or $V^{IV}O(ClO_4)_2$
- solutions of $V^{IV}OSO_4$ or $V^{IV}O(ClO_4)_2$ and maltol to solutions of HSA

Yield similar CD spectra in the visible range. Figure ESI4-2 depicts results of one such experiment.

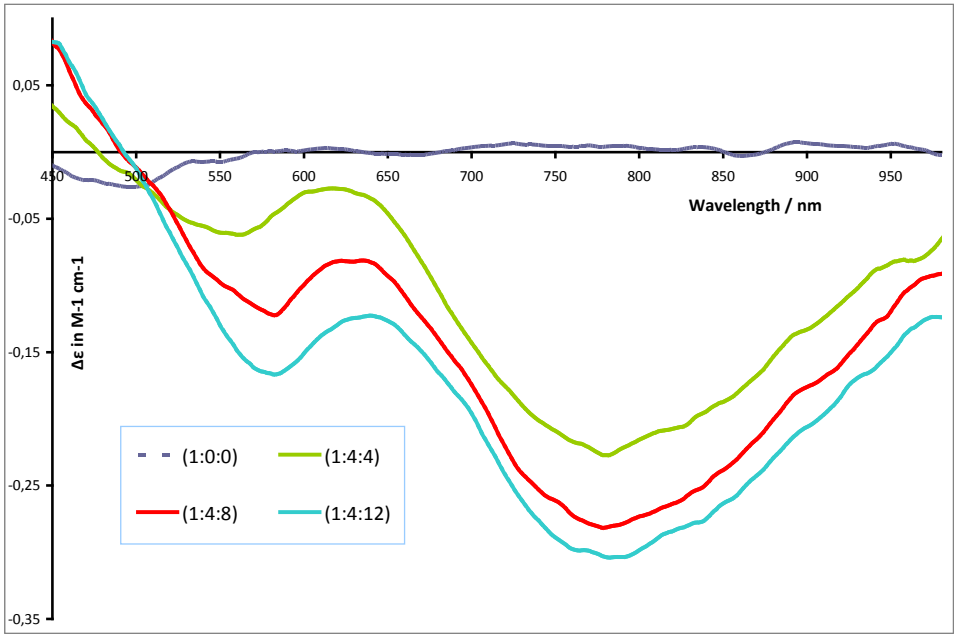

Figure ESI4-4 - CD spectra in the visible range of solutions containing HSA (630 μM) and upon stepwise additions of a solutions containing $V^{IV}O$ and maltol in HEPES-S buffer pH of 7.4. The molar ratios are indicated in the figure.

The CD spectra depicted in Fig. ESI4-4 differ from those of solutions containing HSA and $V^{IV}O$, thus confirming the distinct nature of the $V^{IV}O$ binding modes to HSA when maltol is present.

This journal is © The Royal Society of Chemistry 2012

ESI5 – RT EPR measurements

ESI5-1 – The interaction of HSA with $V^{IV}O$ studied by RT EPR

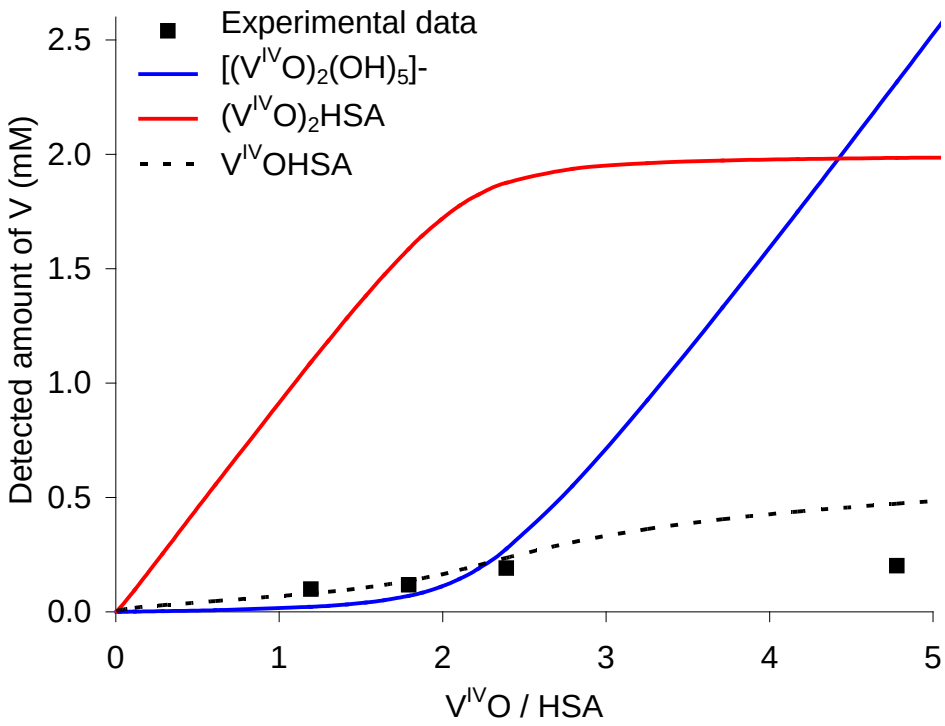

ESI5-1 Comparison of the detected (quantitative RT EPR) amount of $V^{IV}O$ with the speciation in the $V^{IV}O$: HSA (fatted) system (c(HSA)= 1mM)

ESI5-2 – The interaction of HSA with $V^{IV}O(mal)_2$ studied by RT EPR

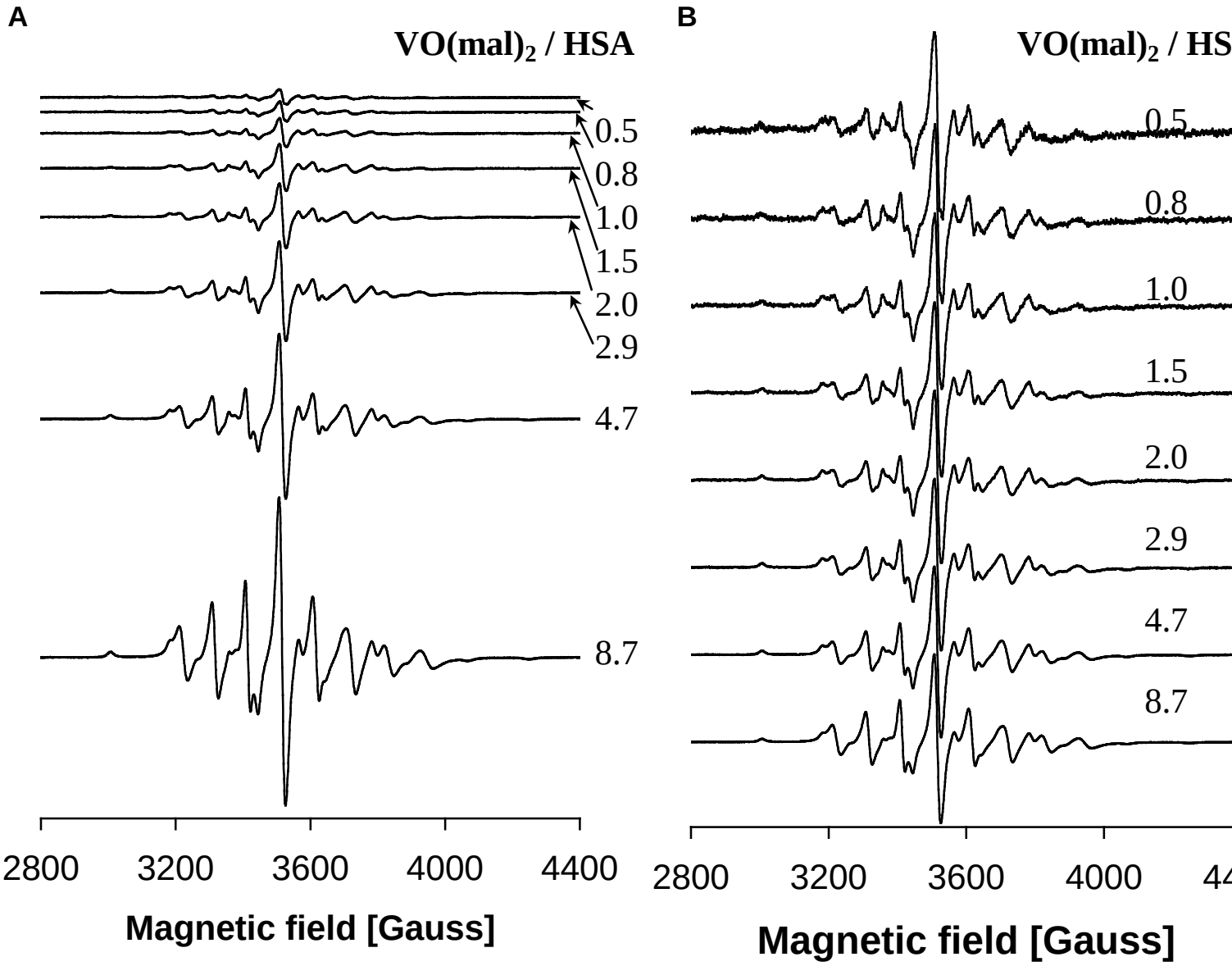

Fig ESI5-2 The measured RT EPR spectra of HSA (1mM) titrated with $V^{IV}O(mal)_2$, the $V^{IV}O(mal)_2$: HSA ratios indicated on the figures. **A** Spectra with original amplitude **B**: Normalized spectra

This journal is © The Royal Society of Chemistry 2012

ESI5-3 – Fitting of the titration of HSA with $V^{IV}O(mal)_2$

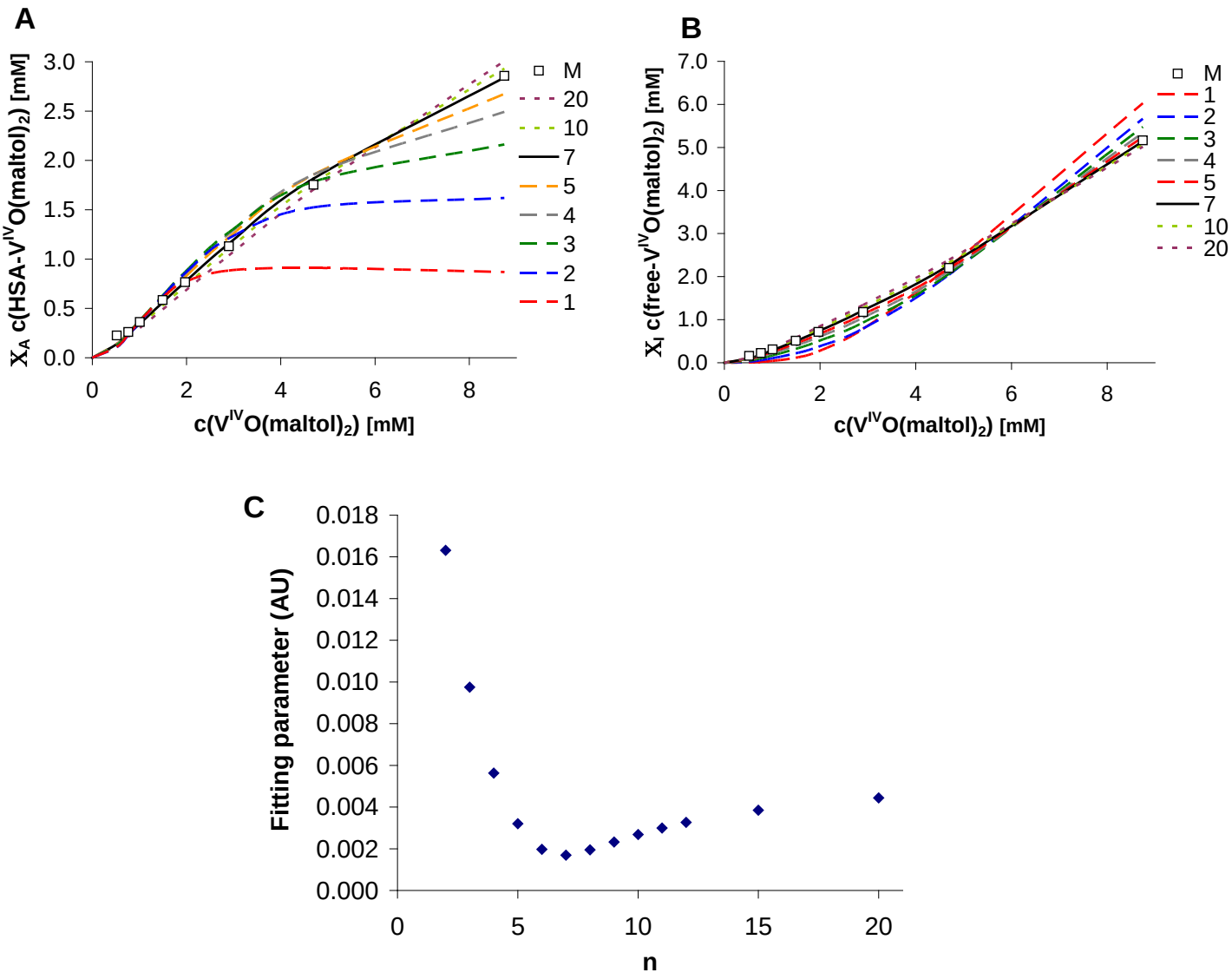

Fig ESI5-3 The determined concentration of the HSA bounded $V^{IV}O$ (axial type spectra, **A**) and the HSA unbounded $V^{IV}O$ (isoropic type spectra, **B**) were fitted with the assumption of different number of equivalent biniding site (n). The measured points (M) indicated with □. The determined fitting parameter in the function of *n* can be seen in **C**.